Analysis of Adaptive Response to Dosing Protocols for Biofilm Control

Analysis of Adaptive Response to Dosing Szomolay, B, Klapper, I. & Dindos, M. 2010, 'Analysis of Adaptive Response to Dosing Protocols for Biofilm Control', Siam Journal on Appied Mathematics, Vol. 70, No. 8, pp. 3175-3202

Analysis of Adaptive Response to Dosing Protocols for Biofilm Control

***Barbara Szomolay*[1], *Isaac Klapper*[2], *Martin Dindos*[3]**

Mathematical Biosciences Institute, The Ohio State University[1]
Department of Mathematical Sciences, Montana State University[2]
Maxwell Institute for Mathematical Sciences, The University of Edinburgh[3]

Abstract

Biofilms are sessile populations of microbes that live within a self-secreted matrix of extracellular polymers. They exhibit extreme tolerance to antimicrobial agents, and experimental evidence indicates that in many instances repeated doses of antimicrobials further reduce efficacy of disinfection due to an adaptive stress response. In this investigation, a mathematical model of bacterial adaptation is presented consisting of an adapted-unadapted population system embedded within a moving boundary problem coupled to a reaction-diffusion equation. The action of antimicrobials on biofilms under different dosing protocols is studied both analytically and numerically. We find the limiting behavior of solutions under periodic and on-off dosing as the period is made very large or very small. In many instances, heavy dosages are undesirable, and our results indicate that on-off dosing for small doses of biocide is more effective than constant dosing. Moreover, in a specific case, on-off dosing for short periods is again more effective regardless of the biocide dose. We also provide sufficient conditions for the eradication of biofilms under constant dosing regimen.

1 Introduction

Biofilms form when sufficient numbers of microorganisms adhere to surfaces in aqueous environments and excrete a slimy, glue-like matrix. It has been estimated that approximately 99 % of bacteria live in biofilm communities and not in a free-living, planktonic state [10]. Biofilms have been found to be involved in a wide variety of microbial infections in the body, by one estimate 80% of all infections [11]. They are also ubiquitous in industrial and civilian contexts including, for example, water distribution and treatment systems [12, 13]. Thus, effective biofilm control agents are highly desirable. There are many available antimicrobial substances that can effectively eradicate planktonic populations and thus would seem to be likely control candidates. However, bacteria living in biofilms are notorious for their recalcitrance: often minimum inhibitory concentrations (MICs) of antimicrobials for bacteria in biofilms are on the order of 10^3 times larger than MICs for the same organisms suspended in planktonic cultures, e.g. [15]. It is in fact believed that there are multiple resistance mechanisms present within a biofilm community, including weak

antimicrobial penetration into the biofilm due to reaction-diffusion barriers and slow growth due to nutrient limitation [16, 17].

The focus of this paper is on a specific stress response to antimicrobial stimulus designated adaptive resistance [17]. We remark that by "adaptive" we do not refer to selective emergence of a genetically distinct, specially resistant strain, but instead to a non-selective phenotypic response (i.e., changed pattern of gene expression) available to a general population when subject to an applied stress [25]. Such a response has been observed in planktonic populations exposed to sub-lethal antimicrobial dosages, e.g. [24]. It is hypothesized in the case of biofilms that, even when exposed to what would be a lethal dosage for a planktonic population, shelter offered to organisms located deeper in the biofilm at least temporarily results in sublethal dosages of antimicrobial thus allowing time for upregulation of adaptive defenses. Examples include induction of genes resulting in upregulation of catalase production in response to hydrogen peroxide [20] and upregulation of beta-lactamases in response to beta-lactam antibiotics [19, 21]. By the way, it is perhaps not surprising that microbes have such defenses in their arsenals as many antimicrobials are derived from the environment and hence not necessarily unfamiliar to their targets. Both of the antimicrobials just mentioned are found in natural environments for example.

While in principal available to planktonic- or biofilm-state organisms, in practice adaptive stress response would seem to be much more effective for biofilm than for planktonic communities. A modeling study of both the biofilm and planktonic culture case indicated that, due to diffusion-reaction barriers, very large increases in dosages would be necessary to prevent adaptive response in thick biofilms [22], suggesting that adaptive response is considerably more dangerous in biofilms than in planktonic populations. Thus we concentrate attention here on biofilms. We note though that a thin biofilm lacks much of a matrix barrier and hence, within the scope of this paper at least, can be considered similar to a planktonic population.

The phenomenon of adaptive response is clearly relevant to dosing strategy. Constant high-dosage treatment, though effective [1], may be expensive, unpractical or even dangerous. An episodal regime thus seems attractive in order to allow reversion to the unadapted state and to allow disinfected material to be cleared between dosages, reducing the reaction-diffusion barrier to antimicrobial access [18]. There is both *in vivo* and *in vitro* evidence to support this conjecture: Karlowsky et al. [32] have shown that the adaptive resistance of Gram-negative bacteria to aminoglycoside develops in immunocompromised patients and showed evidence that a treatment with MIC ratios and once-daily dosing results in the best outcome. This finding is also supported by [33]; dose administration at 24 hour intervals may increase efficacy by allowing time for adaptive resistance to reverse. The advantage of longer dosing intervals for aminoglycosides was studied earlier in [35]. Due to the high MICs required for biofilm control, it is plausible that, given a fixed quantity of antimicrobial and an unwelcome biofilm, a short, high dosage application regime may be preferable to a prolonged, low dosage one. Available evidence is consis-

tent with this hypothesis [6]. Nevertheless, even a very high dose is not sufficient for full disinfection of a thick biofilm if applied for only a short duration due to diffusive-reactive barriers [22]. Hence regrowth (which favors a dosing strategy with short off times or even constant dosing) is to be expected to eventually necessitate further treatment. On the other hand, adaptive responses come at an expense to the microorganisms and hence can be expected to be downregulated at some point (which favors a dosing strategy with long off times) in the absence of antimicrobial antagonism. Development of a long term dosage strategy which balances regrowth and downregulation time scales is hence desirable. Given a fixed average rate of antimicrobial application, is it better to apply a constant dose or a periodic one? If periodic, what should the period be? In between application of high dosages, is it most advantageous to set the dosage to zero in order to encourage downregulation of adaptive resistance? Note that, as already mentioned, one question we do not address concerns the effects of selective pressure on a special, resistant subpopulation; we suppose a single, clonal population throughout.

Choice of dosing interval may be important. The study by Sanderson & Stewart [4] investigated the role of dosing protocols for the biocide monochloramine both mathematically and experimentally. Their model, which did not include any adaptive response mechanism, correctly simulated rapid disinfection followed by steady regrowth. However, it also predicted that, because of a reduction in the reaction-diffusion barrier, a second dose would be more effective than the first dose whereas in actuality the opposite was observed in the experiments, due, presumably, to adaptive response and possibly short intervals between dosings. Adaptive response has been problematic in other dosing studies as well. For example, in [8] investigators observed that efficacy of twice daily, pulsed doses of chlorhexidine (a common active ingredient in mouthwash) applied to dental biofilms decreased dramatically after the first application while in [5], investigators found that insufficiently high dosages of an antimicrobial in a heat exchange system actually seemed to enhance biofilm activity, possibly due to adaptive stimulation of production of extracellular matrix material. These examples and others suggest that if sustained high dosage attack is not practical, dosing strategies need to take into account the possibility of adaptive response defenses.

The objective of this study is to build on a previously introduced biofilm model [22, 9] in order to analyze different dosing protocols with particular focus on the contrast between constant and periodic or on-off dosing regimens. To distinguish between dosing strategies, we define $u(t)$ as the externally applied biocide concentration through the biofilm bulk-fluid interface. The term 'periodic dosing' is used if $u(t)$ is periodic in time t and positive on a set of full measure. The term 'on-off dosing' is used if $u(t)$ is nonnegative periodic and zero on a set of positive measure. In this work, results concerning constant, periodic and on-off dosing strategies against biofilms are presented. In Theorem 1 we present sufficient conditions for the existence of trivial/non-trivial steady-states. In Theorems 2 and 3 the limiting behavior of periodic solutions is studied for large and small periods, which allows us

to directly compare these two dosing strategies with constant dosing. For example, it can be shown that for small doses of biocide, on-off dosing is always more effective than constant dosing and hence should be preferred (see Corollary 3). Numerical simulations indicate that for large doses this might not be true, and constant dosing may be preferable depending on the death rate due to antimicrobial action. For example, in the case when this rate is linear (in biocide), a consequence of Theorem 2 is that on-off dosing for small periods is always better than constant dosing regardless of the biocide dose. On the other hand, as a consequence of Theorem 3 we are able to state sufficient conditions under which the periodic dosing is better or worse than constant dosing. This statement is formulated in Theorem 4. To illustrate the applicability of Theorems 1-2, we did a simple computational dosing experiment which compares the effectiveness of a single dosing with multiple dosing. Our results indicate that the thickness of the biofilm is related to the success of dosing, i.e., at low, medically relevant dosage levels, thin biofilms are better treated with a single dose, whereas it is much harder to treat thick biofilms effectively with either a single dose or multiple doses.

As a final remark, we note the existence of another type of resistance, namely through the so-called persister cell [26]. Persisters are special cells present in microbial populations that, in contrast to adaptive responders [34], exhibit a remarkable general tolerance towards antimicrobials. Their nature is still a subject of investigation. It has been proposed that persisters are, essentially, normal cells that have temporarily changed phenotype into a protective state [27], though other possible explanations exist, e.g. [28, 29]. One phenotype-based theory posits that the transition to and from the persister state is mediated by the presence of an antimicrobial stress [26]. While biologically distinct from adaptive response defenses, this theory of persisters leads to models that are mathematically related and also suggest utility of on-off type dosing regimes [2, 3, 7].

2 The biofilm model

Our model is an extension of a previously proposed 1D moving boundary biofilm model [9] that was linear in the variable B (antimicrobial concentration). Bacterial adaptation was analyzed including growth and detachment. Global existence and other properties of solutions were shown and the corresponding steady-states were studied. In particular, sufficient conditions for the existence of trivial/non-trivial steady-states were established. Here we will replace the linear death rates due to antibiotic action by nonlinear functions φ and ψ. When linear, these terms lead to the unrealistic result that the most optimal dosing strategy is a delta function which, in turn, results in qualitatively incorrect predictions. An appropriate choice of the functions φ and ψ (for example, bounded) removes this problem. This modification does not invalidate the existence results from [9], so the results on the existence of solutions of the PDE system and the corresponding steady-states carry over.

We now describe the mathematical model of the dynamics of antimicrobial concentration, biomass constituents and biofilm thickness. The bacterial population is comprised of the following phenotypes - unadapted cells volume fraction X_u, adapted cells volume fraction X_a, dead unadapted cells volume fraction X_{ud} and dead adapted cells volume fraction X_{ad}. Volume-specific densities are assumed constant. It is assumed for simplicity that there is no substrate limitation (saturation occurs) and that biomass phases can be regarded as incompressible ($X_u + X_{ud} + X_a + X_{ad} = 1$). The equations of the cell volume fractions are then, on spatial domain $x \in [0, L(t)]$,

$$\frac{\partial X_u}{\partial t} + \frac{\partial}{\partial x}(X_u v) = -\underbrace{\varphi(B)X_u}_{\text{death}} - \underbrace{\lambda(B)X_u}_{\text{adaptation}} + \underbrace{\alpha X_u}_{\text{growth}} + \gamma X_a \tag{1}$$

$$\frac{\partial X_{ud}}{\partial t} + \frac{\partial}{\partial x}(X_{ud} v) = \varphi(B)X_u \tag{2}$$

$$\frac{\partial X_a}{\partial t} + \frac{\partial}{\partial x}(X_a v) = \lambda(B)X_u - \underbrace{\psi(B)X_a}_{\text{death}} + \underbrace{\alpha X_a}_{\text{growth}} - \underbrace{\gamma X_a}_{\text{reversion}} \tag{3}$$

$$\frac{\partial X_{ad}}{\partial t} + \frac{\partial}{\partial x}(X_{ad} v) = \psi(B)X_a, \tag{4}$$

where v is the advective velocity driving the convective biomass transport and B is the antimicrobial concentration. The population of unadapted cells in equation (1) changes due to growth, death from antibiotic action, loss from transition to adapted cells, and gain as the adapted cells revert back to unadapted cells. The population of adapted cells in equation (3) changes due to growth, death and loss due to reversion. The dead cell population in equations (2),(4) increases by disinfection of living cells to dead ones. We remark here that the unadapted cell population dies at a faster rate than adapted cells due to the adaptive response, i.e., $\varphi > \psi$. Distinguishing the two dead cell populations (rather than considering them as one) is for bookkeeping purposes only. Note that in the case of adaptation, reversion may be different than for persisters, where reversion is often assumed only in the absence of antibiotics (see [3]). We also assume that the growth rates of unadapted and adapted cells are the same. In actuality, presumably unadapted cells grow faster, though the differences in growth rates seem small (P.S. Stewart, personal communication). This is a significant difference from persisters which are known to be slow growers [30].

We regard our model as dimensionless with t scaled by a typical experimental (or treatment) time τ. It is assumed that living and dead cells react with the biocide at the same rate, i.e., the cell-biocide reactions are independent of viability. That is, we suppose a reactive biocide. Non-reactive biocides are generally similar in behavior because they typically require active targets, which in turn require an active limiting substrate, e.g. oxygen. If the unadapted and adapted cell types react with the biocide at the same rate, then the biocide concentration in dimensional variables is

given by the equation

$$\frac{\partial B}{\partial t} = D\frac{\partial^2 B}{\partial x^2} - kX_0 B,$$

where D is the diffusion rate, k is the biocide-cell reaction rate and X_0 is the (constant) total cell density. It is also assumed that in the biofilm the biocide concentration is quasi-static, i.e., the time derivative $\partial B/\partial t$ can be neglected. If l is a characteristic biofilm thickness, then the previous assumption amounts to assuming that the characteristic time for diffusion $l^2 D^{-1}$ is small compared to the duration of the biocide treatment τ and the other time scales, including $1/\alpha, 1/\gamma, 1/\lambda$.

Biofilm thickness $L(t)$ changes in response to the advective velocity of biomass v and to detachment of biomass. In this model, detachment is treated as a surface erosion of the biofilm at a rate proportional to the square of the biofilm thickness, a standard practice for 1D biofilm models [31]. Summing (1)–(4) and taking into account the incompressibility condition, we obtain a formula for the advection velocity v given by equation (10). Hence, the dimensionless model equations can be rewritten in a simpler fashion

$$\frac{\partial^2 B}{\partial x^2} = \phi^2 B \tag{5}$$

$$\frac{\partial X_u}{\partial t} + v\frac{\partial X_u}{\partial x} = -(\varphi(B) + \lambda(B))X_u + \alpha(1 - X_u - X_a)X_u + \gamma X_a \tag{6}$$

$$\frac{\partial X_{ud}}{\partial t} + v\frac{\partial X_{ud}}{\partial x} = \varphi(B)X_u - \alpha(X_u + X_a)X_{ud} \tag{7}$$

$$\frac{\partial X_a}{\partial t} + v\frac{\partial X_a}{\partial x} = \lambda(B)X_u - \psi(B)X_a + \alpha(1 - X_u - X_a)X_a - \gamma X_a \tag{8}$$

$$\frac{\partial X_{ad}}{\partial t} + v\frac{\partial X_{ad}}{\partial x} = \psi(B)X_a - \alpha(X_u + X_a)X_{ad} \tag{9}$$

$$\frac{\partial v}{\partial x} = \alpha(X_u + X_a) \tag{10}$$

$$\frac{dL}{dt} = v(L, .) - \sigma L^2 \tag{11}$$

again with $x \in [0, L(t)]$. We would like to point out that the detachment term σL^2 could be essentially replaced by any non-negative continuous function $f(L)$, where f grows faster than linear in L.

The parameter ϕ^2, square of the so-called Thiele modulus, is the ratio of the biocide-cell reaction rate kX_0 and the characteristic time of diffusion $l^2 D^{-1}$; it is an indicator of effectiveness of the biocide concentration against the biofilm. In particular, over times short compared to growth and erosion time scales, biofilm thickness is almost constant with, say, approximate thickness l. Since $\sqrt{D/kX_0}$ has units of length, then $1/\phi = \sqrt{D/kX_0}/l$ is approximately the depth in scaled variables of the biofilm layer in which most disinfection occurs (see [22]).

The boundary conditions are

$$\begin{aligned} &\frac{\partial B}{\partial x}(0,t) = 0, \quad B(L(t),t) = u(t) \quad \text{for} \quad 0 \le t \le P \\ &v(0,t) = 0 \quad \text{for} \quad 0 \le t \le P, \end{aligned} \tag{12}$$

where $u(t)$, the externally applied antimicrobial concentration, is a nonnegative piecewise continuous periodic function of period P. It follows directly from (5) and (12) that the biocide concentration is given by

$$B(x,t) = u(t)\frac{\cosh(\phi x)}{\cosh(\phi L(t))}. \tag{13}$$

The function $\lambda(B)$ is defined as

$$\lambda(B) = \begin{cases} \lambda & \text{if } B > 0, \\ 0 & \text{if } B = 0. \end{cases}$$

Note that adaptation only occurs in the presence of biocide. The disinfection rates φ and ψ are monotone increasing, nonnegative and locally Lipschitz with at most polynomial growth such that $\varphi(0) = \psi(0) = 0$ (the linear case was previously studied in [9]). A list of the model parameters is given in Table 1.

ϕ	Thiele modulus
α	maximum specific growth rate
γ	adapted-unadapted cell reversion rate
$\lambda(B)$	unadapted-adapted cell transformation rate
$\phi(B)$	biocide-unadapted cell reaction rate
$\psi(B)$	biocide-adapted cell reaction rate
σ	detachment

Table 1: Model parameters.

In order to explore optimal dosing strategies, we introduce functionals to be optimally minimized with respect to the externally applied antimicrobial concentration $u(t)$. In general, antimicrobials can be bactericidal (killing bacteria, e.g. penicillin) and bacteriostatic (inhibiting the growth of bacteria, e.g. tetracycline). Motivated by these two classifications, we introduce two types of minimizing functionals - functional J (the long-term average of the number of viable organisms roughly speaking) and functional J_L (the long-term average of biofilm thickness), i.e.,

$$J(u) = \lim_{T\to\infty} \frac{1}{T} \int_0^T \int_0^{L(t)} (X_u(x,t) + X_a(x,t)) dx dt \tag{14}$$

and

$$J_L(u) = \lim_{T\to\infty} \frac{1}{T} \int_0^T L(t)dt. \tag{15}$$

Throughout this paper we will assume, when $u(t)$ is periodic, that the system (5)-(11) has a periodic solution satisfying the boundary conditions (12). In fact, numerical simulations suggest that given any initial data, the solution of the system (5)-(11) becomes periodic as $t \to \infty$ with length of period P. This implies that Formulas (14) and (15) simplify to

$$J(u) = \lim_{T\to\infty} \frac{1}{P} \int_T^{T+P} \int_0^{L(t)} (X_u(x,t) + X_a(x,t))dxdt \tag{16}$$

and

$$J_L(u) = \lim_{T\to\infty} \frac{1}{P} \int_T^{T+P} L(t)dt. \tag{17}$$

This form of the functionals is numerically more convenient and will be used throughout

3 Analysis of dosing protocols

We consider three dosing types: constant dosing, periodic dosing and on-off dosing (a special case of periodic dosing). The goal is to find a dosing strategy for which the functionals defined above are minimal. We start with constant dosing by reviewing and generalizing the results from [9]. The other two dosing strategies will be discussed later making use of and extending results obtained for constant dosing.

3.1 Constant dosing

The existence of steady-state solutions for the biofilm model with functions φ and ψ linear has been established in [9]. However all the results from [9] remain true even for the more general functions φ and ψ we allow here. Denote by (S) the system of steady-state equations corresponding to (5)–(10) with boundary conditions

$$\frac{\partial B}{\partial x}(0) = 0, \quad B(L) = u_0, \quad v(0) = 0, \quad v(L) = \sigma L^2. \tag{18}$$

For any $u_0 \geq 0$ there exists at least one solution (possibly the trivial one $L = 0$) of the system (S). In fact, we have sufficient conditions for the existence of trivial/non-trivial steady-states depending on dosage u_0. This is formulated in the following theorem:

Theorem 1. *Given parameters α, γ, σ, λ and functions φ, ψ satisfying the conditions assumed earlier, there exists a number u_{max}, $0 < u_{max} \leq \infty$ such that for any $u_0 \in [0, u_{max})$ there is at least one continuous nontrivial solution of the system (S) satisfying the boundary conditions (18). Let $M_\varphi = \lim_{u\to\infty} \varphi(u)$ and $M_\psi = \lim_{u\to\infty} \psi(u)$. Then $u_{max} = \infty$ if and only if one of these holds:*

- *$M_\varphi < \infty$, $M_\psi = \infty$ and $M_\varphi + \lambda \leq \alpha$*
- *$M_\varphi = \infty$, $M_\psi < \infty$ and $M_\psi + \gamma \leq \alpha$*
- *$M_\varphi < \infty$, $M_\psi < \infty$ and $\Gamma_\infty \leq \alpha$, where*

$$\Gamma_\infty = \frac{M_\psi + \gamma + M_\varphi + \lambda - \sqrt{(M_\psi + \gamma + M_\varphi + \lambda)^2 - 4(M_\psi M_\varphi + \lambda M_\psi + \gamma M_\varphi)}}{2}.$$

Otherwise, u_{max} is a positive number with lower bound $u_{max} \geq \overline{u}$, where $\overline{u}$ is the smallest positive solution of an implicit equation

$$\alpha = \frac{\psi(\overline{u}) + \gamma + \varphi(\overline{u}) + \lambda - \sqrt{\mathcal{F}(\overline{u})}}{2}$$

with $\mathcal{F}(\overline{u}) = (\psi(\overline{u}) + \gamma + \varphi(\overline{u}) + \lambda)^2 - 4(\psi(\overline{u})\varphi(\overline{u}) + \lambda\psi(\overline{u}) + \gamma\varphi(\overline{u}))$.

Remark: Note that the theorem statement does not discuss non-uniqueness of solutions. It has been shown in [9] that the solutions are unique for small doses of biocide u_0, but for large doses non-uniqueness in fact can occur.

Proof. This theorem was proved in the linear case of the functions φ and ψ in [9]. Based on an existence result from [9] the system (S) has a nontrivial continuous solution of length L provided that the autonomous system

$$\begin{aligned} \frac{dx_u}{dt} &= -(\varphi(B_0) + \lambda)x_u + \alpha(1 - x_u - x_a)x_u + \gamma x_a \\ \frac{dx_a}{dt} &= \lambda x_u - \psi(B_0)x_a + \alpha(1 - x_u - x_a)x_u - \gamma x_a \end{aligned} \tag{19}$$

has a positive ($x_u, x_a > 0$) equilibrium. Here $B_0 = \frac{u_0}{\cosh \phi L}$. Analysis of this autonomous system as done in [9] implies that such an equilibrium exists if and only if

$$\alpha > \frac{\psi(B_0) + \gamma + \varphi(B_0) + \lambda - \sqrt{\mathcal{F}(B_0)}}{2}, \tag{20}$$

where $\mathcal{F}$ is the function defined above. If u_0 is small, then so is B_0, as $B_0 \leq u_0$. It follows that for small enough values of u_0 the condition (20) is always satisfied as the expression on the right-hand side is close to zero. From this the existence of nontrivial continuous steady state solutions follows for u_0 on some interval $[0, u_{max})$.

Further examination of condition (20) implies that it will be always satisfied (for arbitrary large u_0) in any of the three cases stated in Theorem 1. Otherwise, the condition yields at least the implicit lower bound $\overline{u}$ on the value of u_{max} as for $u_0 < \overline{u}$ the required condition (20) holds. □

3.2 Periodic and On-off dosing

In this section we consider a different dosing strategy, namely periodic dosing. Of particular interest is the special case of 'on-off dosing' where the dose is applied to the biofilm for a fraction of overall time only and no dose is given for the rest of time. The idea is to provide a 'recovery time' for the biofilm. The presence of biocide causes biofilm to become resistant which is manifested by an increased presence of adapted X_a cells. To counter, we decrease time of presence of biocide which should (and will) lower the formation of adapted cells. This dosing strategy has potential to be better overall than constant dosing.

We introduce the following notation. Let u be a nonnegative, periodic, continuous (or, more generally, piecewise continuous) function with period 1. For any positive number $\omega > 0$ we define the function

$$u^\omega(t) = u(\omega t), \qquad \text{for } t \in \mathbb{R}. \tag{21}$$

Note that u^ω is a periodic function of period $P = 1/\omega$ and, hence, ω is its frequency. Denote by B^ω, X_u^ω, X_{ud}^ω, X_a^ω, X_{ad}^ω, v^ω, L^ω the corresponding periodic solution of the system (5)-(11) with boundary conditions (12). We denote the values of the corresponding functionals by J^ω and J_L^ω, respectively. Let μ be the Lebesgue measure of the set $\{t \in [0,1]; u(t) > 0\}$. It follows that $\mu \in (0,1]$. In the case of on-off dosing, when $u(t)$ is an step function such that $u(t) > 0$ on $[0,\mu]$ and $u(t) = 0$ on $(\mu,1]$, the parameter μ is basically the ratio of the dosing time to the period. From now on we will use the term 'dosing ratio' for the variable μ. Note that the case $\mu = 1$ corresponds to constant dosing, and the case $\mu = 0$ is not defined.

It turns out that we can analyze the limiting behavior of periodic solutions for large and small frequencies. More precisely, in the theorems below we make statements about the limit of the functionals J^ω, J_L^ω as the frequency $\omega \to \infty$ and $\omega \to 0+$. We start with a result relevant to the high frequency case:

Theorem 2. *Let $u_0 = \int_0^1 u(t)dt$. Then any increasing sequence $\omega_1, \omega_2, \omega_3, \ldots$ such that $\omega_n \to \infty$ has a subsequence $(\omega_{n_i})_{i\in N}$ satisfying*

$$L^\infty = \lim_{i\to\infty} L^{\omega_{n_i}}(t) \quad \textit{uniformly for all } t > 0,$$

and all functions $B^{\omega_{n_i}}(x,t)$, $X_a^{\omega_{n_i}}(x,t)$, $X_u^{\omega_{n_i}}(x,t)$, $X_{ad}^{\omega_{n_i}}(x,t)$, $X_{ud}^{\omega_{n_i}}(x,t)$, $v^{\omega_{n_i}}(x,t)$ converge for $x \in [0, L^\infty)$ and $t > 0$ to functions $B^\infty(x)$, $X_a^\infty(x)$, $X_u^\infty(x)$, $X_{ad}^\infty(x)$, $X_{ud}^\infty(x)$, $v^\infty(x)$ that are independent of $t > 0$. In the case of function B^∞ the convergence is only in the weak sense, all other functions converge uniformly in x.

Moreover, these functions satisfy on the interval $[0, L^\infty]$ the equations of a steady-

state solution

$$\frac{\partial^2 B^\infty}{\partial x^2} = \phi^2 B^\infty \tag{22}$$

$$v^\infty \frac{\partial X_u^\infty}{\partial x} = -(\Phi(B^\infty) + \mu\lambda)X_u^\infty + \alpha(1 - X_u^\infty - X_a^\infty)X_u^\infty + \gamma X_a^\infty \tag{23}$$

$$v^\infty \frac{\partial X_{ud}^\infty}{\partial x} = \Phi(B^\infty)X_u^\infty - \alpha(X_u^\infty + X_a^\infty)X_{ud}^\infty \tag{24}$$

$$v^\infty \frac{\partial X_a^\infty}{\partial x} = \mu\lambda X_u^\infty - \Psi(B^\infty)X_a^\infty + \alpha(1 - X_u^\infty - X_a^\infty)X_a^\infty - \gamma X_a^\infty \tag{25}$$

$$v^\infty \frac{\partial X_{ad}^\infty}{\partial x} = \Psi(B^\infty)X_a^\infty - \alpha(X_u^\infty + X_a^\infty)X_{ad}^\infty \tag{26}$$

$$\frac{\partial v^\infty}{\partial x} = \alpha(X_u^\infty + X_a^\infty) \tag{27}$$

$$v^\infty(L^\infty, .) = \sigma(L^\infty)^2 \tag{28}$$

with the boundary condition $B^\infty(L^\infty) = u_0$. *Here the functions* Φ *and* Ψ *are defined by*

$$\Phi(z) = \int_0^1 \varphi\left(\frac{u(t)}{u^0}z\right)dt \quad \textit{and} \quad \Psi(z) = \int_0^1 \psi\left(\frac{u(t)}{u^0}z\right)dt. \tag{29}$$

Finally, values of the functionals $J^{\omega_{n_i}}$ *and* $J_L^{\omega_{n_i}}$ *converge to*

$$J^\infty = \lim_{i\to\infty} J^{\omega_{n_i}} = \int_0^{L^\infty} (X_a^\infty + X_u^\infty)dx, \qquad J_L^\infty = \lim_{i\to\infty} J_L^{\omega_{n_i}} = L^\infty. \tag{30}$$

Remark: Note that if φ is linear, then $\varphi = \Phi$ and the same is also true for ψ. It follows that Φ and Ψ are locally Lipschitz, increasing functions and $\Phi(0) = \Psi(0) = 0$. In the case of the on-off dosing we study below, the function $u(t)$ is defined as u_0/μ on the interval $[0, \mu]$ and zero on $(\mu, 1]$. Hence, $\Phi(z) = \mu\varphi(z/\mu)$ and $\Psi(z) = \mu\psi(z/\mu)$.

Proof. All functions L^{ω_n} are uniformly bounded from above by $\frac{\alpha}{\sigma}$ (c.f. Lemma 2 of [9]). Indeed, if $L(t) > \frac{\alpha}{\sigma}$, then

$$\frac{dL}{dt} = v(L) - \sigma L^2 < \alpha L - \sigma\frac{\alpha}{\sigma}L = 0,$$

which implies that for sufficiently large t we have $L(t) \le \frac{\alpha}{\sigma}$. In our case, we consider periodic solutions. If we had that $L(0) > \frac{\alpha}{\sigma}$, it would follow that $L(P) < L(0)$ (where P is the period of our solution) which is a contradiction. Hence, $L(t) \le \frac{\alpha}{\sigma}$ for all $t \ge 0$.

We can also get an uniform bound on $\frac{dL^{\omega_n}}{dt}$. (11) implies

$$-\frac{\alpha^2}{\sigma} \le -\sigma(L^{\omega_n}(t))^2 \le \frac{dL^{\omega_n}}{dt} = v(L^{\omega_n}) - \sigma(L^{\omega_n})^2 \le v(L^{\omega_n}) \le \alpha L^{\omega_n}(t) \le \frac{\alpha^2}{\sigma}.$$

Hence the functions L^{ω_n} are uniformly Lipschitz in t, i.e., also equicontinuous. By the Ascoli theorem there exist subsequence (n_i) such that the sequence of functions $L^{\omega_{n_i}}$ is convergent. Since the length of the period goes to zero the limit must be a constant function which we call L^∞. If this limit is zero, the proof is complete – in this case $L^\infty = 0$ which corresponds to the trivial steady state solution.

The alternative case is more interesting. It follows from above that L^∞ is constant in t. Since the functions $B^{\omega_{n_i}}$ are explicitly determined by $L^{\omega_{n_i}}$, we have that

$$\frac{\cosh(\phi x)}{\cosh(\phi L^{\omega_{n_i}}(t))} \to \frac{\cosh(\phi x)}{\cosh(\phi L^\infty)} \quad \text{uniformly in } x$$

and

$$u^{\omega_{n_i}}(t) \to u_0 \quad \text{weakly, i.e., for any } \psi \in C_0^\infty(R): \quad \int u^{\omega_{n_i}}(t)\psi(t)dt \to u_0 \int \psi(t)dt,$$

as $\omega_{n_i} \to \infty$. This follows immediately from the fact that u_0 is the average value of each function u^ω. From this the product function $B^{\omega_{n_i}}(x,t) = u(t)\frac{\cosh(\phi x)}{\cosh(\phi L^{\omega_{n_i}}(t))}$ will converge weakly to $B^\infty(x) = u_0\frac{\cosh(\phi x)}{\cosh(\phi L^\infty)}$, where the weak convergence is understood in t, as defined above.

Now for each ω_{n_i} let us introduce new variables which we denote by $\widetilde{B}^i$, $\widetilde{v}^i$, $\widetilde{X}^i_u$, $\widetilde{X}^i_a$, $\widetilde{X}^i_{ud}$, $\widetilde{X}^i_{ad}$ that will only be functions of variable x and not of t. We will define them on the interval $[0, \widetilde{L}^i]$, where

$$\widetilde{L}^i = \inf_t L^{\omega_{n_i}}(t).$$

It follows immediately that $\widetilde{L}^i \to L^\infty$ as $i \to \infty$. The mentioned functions are defined via averaging over the period, which for index i is $\omega_{n_i}^{-1}$, i.e.,

$$\begin{aligned}
\widetilde{X}^i_a(x) &= \omega_{n_i}\int_0^{1/\omega_{n_i}} X_a^{\omega_{n_i}}(x,t)dt,\ \widetilde{X}^i_{ad}(x) = \omega_{n_i}\int_0^{1/\omega_{n_i}} X_{ad}^{\omega_{n_i}}(x,t)dt,\\
\widetilde{X}^i_u(x) &= \omega_{n_i}\int_0^{1/\omega_{n_i}} X_u^{\omega_{n_i}}(x,t)dt,\ \widetilde{X}^i_{ud}(x) = \omega_{n_i}\int_0^{1/\omega_{n_i}} X_{ud}^{\omega_{n_i}}(x,t)dt,\\
\widetilde{B}^i(x) &= \omega_{n_i}\int_0^{1/\omega_{n_i}} B^{\omega_{n_i}}(x,t)dt,\ \widetilde{v}^i(x) = \omega_{n_i}\int_0^{1/\omega_{n_i}} v^{\omega_{n_i}}(x,t)dt. \qquad (31)
\end{aligned}$$

To obtain equations that will be satisfied by these new functions, we will integrate equations (5)-(10) over the interval $[0, \omega_{n_i}^{-1}]$ and average (i.e., multiply by ω_{n_i}). We have

$$\widetilde{B}^i(x) = \omega_{n_i} \int_0^{1/\omega_{n_i}} u(t) \frac{\cosh(\phi x)}{\cosh[\phi L^{\omega_{n_i}}(t)]} dt = u_0 \frac{\cosh(\phi x)}{\cosh[\phi \widetilde{L}^i]} + e_1, \tag{32}$$

$$\widetilde{v}^i \frac{\partial \widetilde{X}^i_u}{\partial x} = -(\Phi(\widetilde{B}^i) + \mu\lambda)\widetilde{X}^i_u + \alpha(1 - \widetilde{X}^i_u - \widetilde{X}^i_a)\widetilde{X}^i_u + \gamma \widetilde{X}^i_a + e_2 \tag{33}$$

$$\widetilde{v}^i \frac{\partial \widetilde{X}^i_{ud}}{\partial x} = \Phi(\widetilde{B}^i)\widetilde{X}^i_u - \alpha(\widetilde{X}^i_u + \widetilde{X}^i_a)\widetilde{X}^i_{ud} + e_3 \tag{34}$$

$$\widetilde{v}^i \frac{\partial \widetilde{X}^i_a}{\partial x} = \mu\lambda \widetilde{X}^i_u - \Psi(\widetilde{B}^i)\widetilde{X}^i_a + \alpha(1 - \widetilde{X}^i_u - \widetilde{X}^i_a)\widetilde{X}^i_a - \gamma \widetilde{X}^i_a + e_4 \tag{35}$$

$$\widetilde{v}^i \frac{\partial \widetilde{X}^i_{ad}}{\partial x} = \Psi(\widetilde{B}^i)\widetilde{X}^i_a - \alpha(\widetilde{X}^i_u + \widetilde{X}^i_a)\widetilde{X}^i_{ad} + e_5 \tag{36}$$

$$\frac{\partial \widetilde{v}^i}{\partial x} = \alpha(\widetilde{X}^i_u + \widetilde{X}^i_a) \tag{37}$$

$$0 = v(\widetilde{L}^i, .) - \sigma[\widetilde{L}^i]^2 + e_6. \tag{38}$$

Here $e_1, e_2, \ldots, e_6$ are the error terms that arise from nonlinear terms. We do not write all of them explicitly, but as an example we look in detail at

$$\begin{aligned} \omega_{n_i} \int_0^{1/\omega_{n_i}} v^{\omega_{n_i}} \frac{\partial X_u^{\omega_{n_i}}}{\partial x} dt &= \omega_{n_i} \int_0^{1/\omega_{n_i}} \widetilde{v}^i \frac{\partial X_u^{\omega_{n_i}}}{\partial x} dt + \omega_{n_i} \int_0^{1/\omega_{n_i}} (v^{\omega_{n_i}} - \widetilde{v}^i) \frac{\partial X_u^{\omega_{n_i}}}{\partial x} dt \\ &= \widetilde{v}^i \frac{\partial \widetilde{X}^i_u}{\partial x} + e, \end{aligned}$$

where $|e| \leq \|\widetilde{v}^i - v^{\omega_{n_i}}\|_\infty \left\| \frac{\partial \widetilde{X}_u^{\omega_{n_i}}}{\partial x} \right\|_\infty$.

We also look at the origin of the functions Φ and Ψ. Consider for example the term $\varphi(B^{\omega_{n_i}})X_u^{\omega_{n_i}}$ in the equation (6). After averaging we obtain

$$\omega_{n_i} \int_0^{1/\omega_{n_i}} \varphi(B^{\omega_{n_i}}) X_u^{\omega_{n_i}} dt = \omega_{n_i} \int_0^{1/\omega_{n_i}} \varphi(B^{\omega_{n_i}}) \widetilde{X}^i_u dt + e', \tag{39}$$

where

$$|e'| = \omega_{n_i} \left| \int_0^{1/\omega_{n_i}} \varphi(B^{\omega_{n_i}})(X_u^{\omega_{n_i}} - \widetilde{X}^i_u) dt \right| \leq C(\|B^{\omega_{n_i}}\|_\infty) \|\widetilde{X}^i_u - X_u^{\omega_{n_i}}\|_\infty.$$

Working further with (39) we see that

$$\omega_{n_i} \int_0^{1/\omega_{n_i}} \varphi(B^{\omega_{n_i}}) \widetilde{X}^i_u dt = \widetilde{X}^i_u \, \omega_{n_i} \int_0^{1/\omega_{n_i}} \varphi\left(u^{\omega_{n_i}}(t) \frac{\cosh(\phi x)}{\cosh(\phi \widetilde{L}^i)} \right) dt + e'', \tag{40}$$

where

$$|e''| = \omega_{n_i} |\widetilde{X}^i_u| \left| \int_0^{1/\omega_{n_i}} \left(\varphi\left(u^{\omega_{n_i}}(t) \frac{\cosh(\phi x)}{\cosh(\phi L^{\omega_{n_i}})} \right) - \varphi\left(u^{\omega_{n_i}}(t) \frac{\cosh(\phi x)}{\cosh(\phi \widetilde{L}^i)} \right) \right) dt \right|.$$

The fact that φ is Lipschitz allows a bound $|e''| \leq C\|L^{\omega_{n_i}} - \widetilde{L}^i\|_\infty$. After change of variables the first term of (40) becomes

$$\widetilde{X}^i_u \int_0^1 \varphi\left(u(t)\frac{\cosh(\phi x)}{\cosh(\phi\widetilde{L}^i)}\right)dt = \widetilde{X}^i_u \Phi\left(u_0\frac{\cosh(\phi x)}{\cosh(\phi\widetilde{L}^i)}\right) = \widetilde{X}^i_u\Phi(\widetilde{B}^i(x)). \tag{41}$$

Similar estimates are worked out for all other nonlinear terms. In total we obtain

$$\begin{aligned} |e_1| + \cdots + |e_6| \;&\leq\; C\|\widetilde{L}^i - L^{\omega_{n_i}}\|_\infty + C\|\widetilde{v}^i - v^{\omega_{n_i}}\|_\infty \left\|\frac{\partial \widetilde{X}^i_\cdot}{\partial x}\right\|_\infty \\ &+\; C(\|B\|_\infty)\|\widetilde{X}^i_\cdot - X^{\omega_{n_i}}_\cdot\|_\infty. \end{aligned} \tag{42}$$

Here $\widetilde{X}^i_\cdot$ represents all variables $\widetilde{X}^i_a$, $\widetilde{X}^i_u$ etc. Let us also remark that the terms $\mu\lambda$ in equations (33) and (35) occur because the original equations only contain λ when $u(t) > 0$, which happens on a set of size μ.

What follows relies on the following technical lemma:

Lemma 1. *There exists a constant $K > 0$ depending only on constants $\alpha, \phi, \lambda, \gamma, \sigma$ and $\|u\|_\infty$ such that the periodic solutions of (5)-(11) are Lipschitz continuous in variable x with Lipschitz constant at most K, that is*

$$\max\left\{\left\|\frac{\partial X_a}{\partial x}\right\|_\infty, \left\|\frac{\partial X_{ad}}{\partial x}\right\|_\infty, \left\|\frac{\partial X_u}{\partial x}\right\|_\infty, \left\|\frac{\partial X_{ud}}{\partial x}\right\|_\infty\right\} \leq K. \tag{43}$$

The crucial part of the claim in this Lemma is that the bound on the Lipschitz norm is uniform and only depends on the constants and L^∞ norm of u. We will not include the proof; this Lemma is closely connected with the question of existence of periodic solutions for which we also did not include the proof. However, the proof would go the same as a similar proof that establishes that the steady state solution is also Lipschitz in x. We did not do it explicitly, as it was not necessary, but in the last part of the proof of the existence of steady state solution we derived an estimate on the distance ρ of two steady state solutions in the form $\frac{d\rho}{dx} \leq F(\rho)$. A slight modification of this estimate provides a uniform bound on the $\frac{d}{dx}$ derivative of the solution, which implies the function is Lipschitz.

To return to our proof, once we have these estimates, we use (6)-(9) to conclude that for some M independent of i we also have that

$$\max\left\{\left\|\frac{\partial X^{\omega_{n_i}}_a}{\partial t}\right\|_\infty, \left\|\frac{\partial X^{\omega_{n_i}}_{ad}}{\partial t}\right\|_\infty, \left\|\frac{\partial X^{\omega_{n_i}}_u}{\partial t}\right\|_\infty, \left\|\frac{\partial X^{\omega_{n_i}}_{ud}}{\partial t}\right\|_\infty\right\} \leq M. \tag{44}$$

Using the fact that functions X^ω_a, X^ω_u, X^ω_{ad} and X^ω_{ud} are periodic in t with period $\omega^{-1}_{n_i}$, we then conclude that the oscillation (difference between sup and inf values) of these four functions is at most $M\omega^{-1}_{n_i} \to 0$ as $i \to \infty$. It follows from (42) that

$$|e_1| + \cdots + |e_5| \leq C\omega^{-1}_{n_i}, \tag{45}$$

where C is a constant depending only on the parameters of the equation and $\|u\|_\infty$.

Now we choose a subsequence a second time. Equations (33), (35) and (37) appear exactly like those equations for a steady state solution we studied closely before, plus some error terms. As we have shown, the solutions of these equation are all uniformly bounded and equicontinuous (Lemma 6.1), and hence by the Ascoli Theorem there is a convergent subsequence as $i \to \infty$. On the other hand, as $i \to \infty$ the error terms vanish and hence, the limit of this subsequence satisfies exactly the equations for steady-state solution. Let us call this limit $X_u^\infty, X_a^\infty, v^\infty$. The domain of these functions is the interval $[0, L^\infty)$.

So far we have uniform convergence of $\widetilde{X}_u^{i_j}$ to X_u^∞, of $\widetilde{X}_a^{i_j}$ to X_a^∞ and of $\widetilde{v}^{i_j}$ to v^∞, where $(i_j)_{j\in N}$ is the selected subsequence. Recalling (44), we can drop the tilde and also see that $X_u^{\omega_{n_{i_j}}}(x,t)$ converges to $X_u^\infty(x)$ uniformly for arbitrary t (and similarly for other functions). This is the desired subsequence. □

Remark: It is possible that two different subsequences converge to two different limits. This only happens though if there is non-uniqueness of steady-state solutions. Otherwise, the limit is necessarily unique.

Now we have a look at the other limit $\omega \to 0+$, i.e., dosing time scale long compared to other time scales in the problem. In this case the length of period goes to infinity. We will formulate the upcoming theorem in the simplest case that for each u_0 there is a single nonzero steady-state solution. This theorem can be modified for the more general case in a straightforward manner. We, however, choose not to do so in order to keep the proof reasonably short.

Theorem 3. *Let $u(t)$ be a periodic piecewise continuous function of period 1 and consider as in (21) the functions u^ω of period $1/\omega$ and their corresponding periodic solutions B^ω, X_u^ω, X_{ud}^ω, X_a^ω, X_{ad}^ω, v^ω, L^ω of the system (5)-(11). Assume that for each $u_0 \in \{u(t);\, t \in \mathbb{R}\}$ there is a unique nonzero continuous steady-state solution with boundary condition $B(L) = u_0$. Let $J(u_0)$ and $J_L(u_0)$ be the values of the two functionals (14)-(15) for this steady-state solution. Then*

$$\begin{aligned}\lim_{\omega\to 0+} J^\omega &= \lim_{\omega\to 0+} \omega \int_0^{1/\omega}\int_0^{L^\omega(t)} (X_a^\omega(x,t) + X_u^\omega(x,t))dxdt = \int_0^1 J(u(t))dt,\\ \lim_{\omega\to 0+} J_L^\omega &= \lim_{\omega\to 0+} \omega \int_0^{1/\omega} L^\omega(t)dt = \int_0^1 J_L(u(t))dt. \end{aligned} \tag{46}$$

Remark: In the special case of the on-off dosing for the function $u(t) = u_0/\mu$ on $[0,\mu]$ and $u(t) = 0$ on $(\mu, 1]$ these two formulas simplify to

$$\lim_{\omega\to 0+} J^\omega = \mu J(u_0/\mu) + (1-\mu)\frac{\alpha}{\sigma}, \quad \lim_{\omega\to 0+} J_L^\omega = \mu J_L(u_0/\mu) + (1-\mu)\frac{\alpha}{\sigma}. \tag{47}$$

Proof. Assume first that u is continuous. Since $\omega \to 0+$ means that the length of period goes to infinity and since u is a periodic function, it follows that the

stretched function u^ω is extremely slowly varying, i.e., given $\varepsilon > 0$ and an arbitrary large $M > 0$ one can find sufficiently small $\omega > 0$ such that

$$|u^\omega(t+\tilde{t}) - u^\omega(t)| < \varepsilon, \qquad \text{for all } t \in \mathbb{R} \text{ and } |\tilde{t}| < M.$$

Hence, for any fixed t the function u^ω on the large interval $[t-M, t+M]$ is almost constant and approximately equal to $u^\omega(t)$. What this means is that regardless of the values of X_u^ω, X_a^ω, L^ω at time $t-M$, as the time progresses to t, these functions will be closer and closer to the values of functions for the steady-state solution with boundary value $u^\omega(t)$. Recall that we assume there is a unique stable nonzero steady state solution with this boundary condition. Therefore, the same will be true about the values of functionals J and J_L, i.e., for some small $\delta > 0$ at time t:

$$\begin{aligned} \left| \int_0^{L^\omega(t)} (X_a^\omega(x,t) + X_u^\omega(x,t))dx - J(u^\omega(t)) \right| &< \delta, \\ |L^\omega(t) - J_L(u^\omega(t))| &< \delta. \end{aligned} \tag{48}$$

Here δ depends on ω and $\delta \to 0+$ as $\omega \to 0+$. Once we have this estimate, we integrate over the time interval $[0, 1/\omega]$ and average (divide by $1/\omega$) to obtain

$$\begin{aligned} \left| \omega \int_0^{1/\omega} \int_0^{L^\omega(t)} (X_a^\omega(x,t) + X_u^\omega(x,t))dxdt - \omega \int_0^{1/\omega} J(u^\omega(t))dt \right| &< \delta, \\ \left| \omega \int_0^{1/\omega} L^\omega(t)dt - \omega \int_0^{1/\omega} J_L(u^\omega(t))dt \right| &< \delta. \end{aligned}$$

Now, we realize that $\omega \int_0^{1/\omega} J(u^\omega(t))dt = \int_0^1 J(u(t))dt$ and $\omega \int_0^{1/\omega} J_L(u^\omega(t))dt = \int_0^1 J_L(u(t))dt$ and hence, the conclusion (46) holds.

If u is only piecewise continuous the only modification comes at the jump points of functions u. Here briefly for some fixed time period T_0 the value of functionals might differ significantly from the steady state solution. However, as the total period T goes to infinity, the ratio $T_0/T \to 0$, hence in the long run this jump does not matter. □

If follows from Theorem 3 that, in the limit $\omega \to 0$, it is the concavity/convexity of the function $J(u)$ that determines whether or not periodic dosing is better than constant dosing.

Theorem 4. *Let J be the function defined in Theorem 3, that is $J(u)$ is the value of the functional (14) for the steady state solution with constant dose u. Assume that J is a concave down function on the interval $[A_1, A_2]$ and $u(t) \in [A_1, A_2]$. Then*

$$\lim_{\omega \to 0_+} J_\omega = \int_0^1 J(u)dt < J(u_0), \tag{49}$$

i.e., for sufficiently small frequencies ω, periodic dosing is more effective than the constant dosing with dose u_0. Conversely, if J is concave up on the whole interval $[A_1, A_2]$ and $u(t) \in [A_1, A_2]$, then for sufficiently small frequencies ω, periodic dosing is sure to be worse than constant dosing with dose u_0. Similar claims also hold for the functional J_L.

Proof. We expand J around u_0 using Taylor formula, i.e.,

$$J(u) = J(u_0) + J'(u_0)(u - u_0) + \frac{J''(\xi_u)}{2}(u - u_0)^2,$$

where ξ_u is some number in the interval between u and u_0. Next, we replace u by $u(t)$ and integrate J over interval $[0, 1]$.

$$\lim_{\omega \to 0_+} J_\omega = \int_0^1 J(u(t))dt = J(u_0) + \int_0^1 \frac{J''(\xi_u(t))}{2}(u(t) - u_0)^2 dt. \tag{50}$$

The claim then follows; if $J'' < 0$, the right-hand side is smaller than $J(u_0)$ for small values of ω. On the other hand, if $J'' > 0$, the opposite is true. □

Examples of functionals J, J_L that are concave up and down for all u are shown in Figure 1a) and Figure 1b), respectively. As a consequence of Theorem 4, we have the following corollary.

Corollary 1. *Let $J(u)$ be the value of the functional (14) for the steady state solution with constant dose u. If for all u we have $J(u) > 0$, then J is a concave up function for sufficiently large values of u; hence periodic dosing for large doses and small frequencies is less effective than constant dosing.*

Remark: The significance of this observation is the following: $J'' < 0$ (or $J_L'' < 0$) signifies that an increase in dosage is surprisingly effective in the sense that the rate of decrease of J (or J_L) is greater than rate of increase of u, for example, because antimicrobial penetration suffers from diffusive-reactive barriers. In this case it is best to vary dosage in time so as, at least for short times, to expose the biofilm to the particularly effective higher dosages even at the expense of using lower dosages at other times. In the reverse case $J'' > 0$ (or $J_L'' > 0$), the opposite is true – relative ineffectiveness of higher dosing (due for example to antimicrobial saturation) does not justify use of variable dosing. According to Corollary 1, for recalcitrant biofilms such that $J(u) > 0$ for all u, constant application is optimal for large enough dosage.

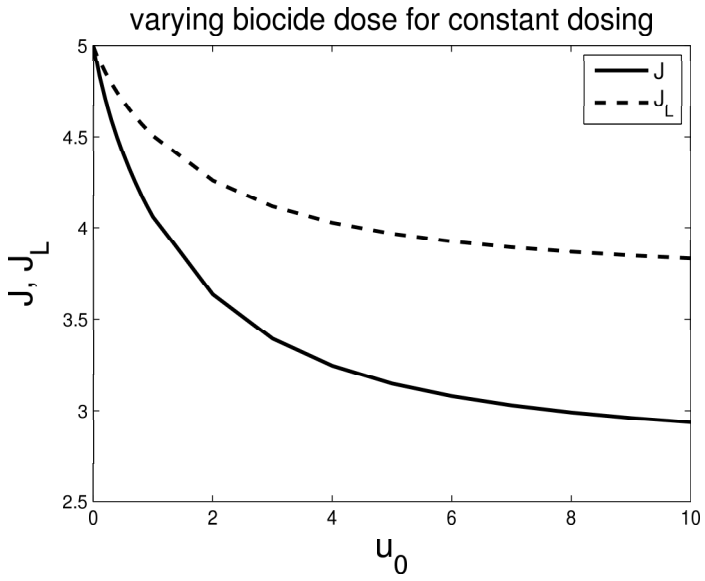

(a)

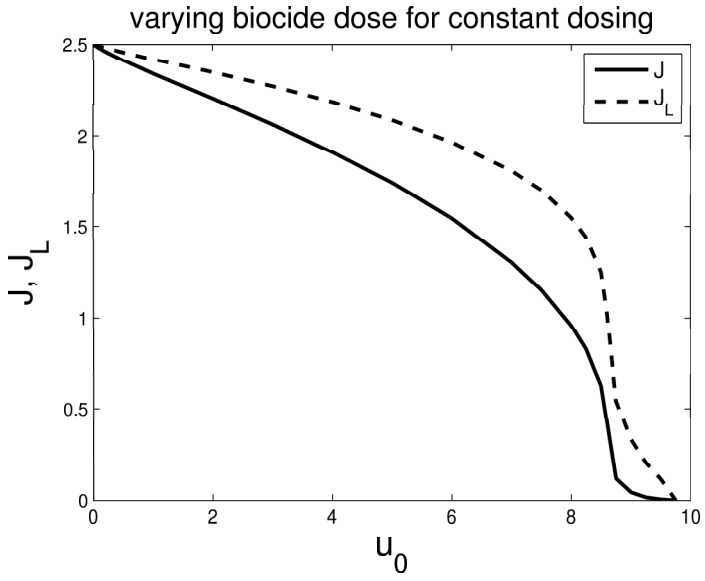

(b)

Figure 1: a) Concave-up functionals J and J_L for different values of the biocide dose u_0 for constant dosing. The values of the parameters are $L(0) = 5, \phi = 1, \lambda = 1, \alpha = 1, \gamma = 0.1, \sigma = 0.2, M_\psi = 0.2, k = 0.1, M_\phi = 2$. b) Concave-down functionals J and J_L for different values of the biocide dose u_0 for constant dosing. The values of the parameters are $L(0) = 2.5, \phi = 1, \lambda = 0.1, \alpha = 1, \gamma = 0.01, \sigma = 0.4$ and the functions ϕ, ψ are chosen to be $\phi(B) = B, \psi(B) = B$.

4 Simulated dosing experiments

Section 4.1 describes numerical methods used in simulations. Section 4.2 presents two important assertions concerning on-off dosing (Corollary 2–3) and finally, Section 4.3 presents an example application dosing experiment where the effects of one dose and two doses are compared.

4.1 Numerical details

So far, parameter choices have been arbitrary up to some mild requirements. For numerical purposes we now specify the functions φ, ψ to be $\varphi(B) = \frac{M_\varphi B}{B+k}$, $\psi(B) = \frac{M_\psi B}{B+k}$ (standard saturation forms). We note here that if the growth rates α_u and α_a for the unadapted and adapted cells differ, for $u_0 = 0$ the biofilm thickness L is only controlled by α_u. On the other hand, for significant doses u_0, the biofilm thickness L in most cases is only controlled by α_a. We will thus continue to set $\alpha_u = \alpha_a$. In actuality, α_u is probably slightly larger than α_a as adaptation mechanisms come with some cost, but a small difference is not of much effect here.

We make estimates as follows for the ratios α/γ, λ/γ and α/σ in case of adaptation based on experimental observations (P. S. Stewart, personal communication). It is estimated that the reversion rate γ is 0.01 to 1 times the growth rate α consistent with observations, e.g [32, 33]. However, in the case when the adapted cells are not killed by the biocide ($M_\psi = 0$), the only relevant case for our model is $\alpha/\gamma = o(1)$. Otherwise, if $\alpha \gg \gamma$ and $M_\psi = 0$, the biocide would have negligible effect on the biofilm thickness, that is to say, it would hardly function as a biocide at all and thus not be of interest practically. Indeed, it can be shown that for $u_0 = 0$ the steady-state solutions satisfy $X_u + X_a = 1$ and $L = \frac{\alpha}{\sigma}$ while when $u_0 \to \infty$, it can be shown that $X_u + X_a \geq 1 - \frac{\gamma}{\alpha}$ and $L \geq \frac{\alpha-\gamma}{\sigma}$, i.e., the biofilm thickness almost does not change compared to no dosing if γ/α is much less than 1. The ratio λ/γ of reversion to disinfection rates has influence on the relative population sizes of the viable cells. For small biocide doses it is easy to show that $X_u \approx \frac{\gamma}{\lambda+\gamma}$ and $X_a \approx \frac{\lambda}{\lambda+\gamma}$, i.e., $X_a/X_u \approx \lambda/\gamma$. Disinfection of unadapted cells may typically require about 1-2 hours, whereas reversion of adapted cells seems to need about 10 hours. Hence, the ratio λ/γ is 0.1-0.2. Finally, we take the detachment coefficient to be 0.1-0.2 times the growth rate α.

The simulations to follow use a second order explicit Runge-Kutta method. Our approach is motivated by techniques used to prove the existence and uniqueness of solutions of the PDE system in [9], and, hence, is based on the method of characteristics. Eq. (1) can be rewritten as

$$\frac{\partial X_u}{\partial t} + \frac{\partial X_u}{\partial x} v = -X_u \frac{\partial v}{\partial x} - (\varphi(B) + \lambda(B))X_u + \alpha X_u + \gamma X_a. \tag{51}$$

The left hand-side in (51) is the directional derivative of X_u in the x, t plane in

the direction $(v, 1)$. The flow of the vector field $(v, 1)$ defines characteristics with characteristic equations

$$\frac{dx}{dt} = v(x(t), t), \quad x(0) = x_0.$$

The time-axis $x = 0$ is also a characteristic, since $v(0, t) = 0$. Hence, the left-boundary conditions for the solutions can be obtained from the method directly. We observe that with passing time the distance between characteristics will increase. If we let this happen for sufficiently long time, we will lose precision since distances between points on the moving grid will increase. To avoid this, we introduce a new characteristic at the moment when the distance between the original characteristics is greater than $2d$, where d is the initial step-size of space. We compute the initial values on the new characteristic using second order interpolation.

Since we have a moving boundary, the velocity at the interface at time i is computed as the weighted average value of the velocities $v(i, j-1)$ and $v(i, j)$ for some appropriate index j such that $x(i, j-1)$ is the closest point on the characteristic at time i to the left of $L(i)$ and $x(i, j)$ is on a characteristic to the right of the interface $L(i)$. Note that the equation for L is $\dot{L} = v(L, .) - \sigma L^2$. Hence, in the case $\sigma = 0$ (no detachment) L would just be a characteristic. When $\sigma > 0$, $L(i)$ is always to the left of the last grid point $x(i, j)$, so $L(i)$ is computed via interpolation (no extrapolation is required).

4.2 Comparing simulation and analytical results

As already mentioned in Section 2, if u is periodic, then the solutions of the system (5)–(11) become periodic as $t \to \infty$ with the same length of period as the function u. In some cases, depending on the parameters, the limiting solution can be nonzero; in other cases, only the trivial limit occurs. This is demonstrated in Figures 2a) and 3a), where the biofilm thickness L is shown for on-off dosing ($u(t) = u_0/\mu$ on $[0, \mu)$ and $u(t) = 0$ on $[\mu, 1)$) with frequency $\omega = 1$ and average biocide dose $u_0 = 49$ and $u_0 = 50$, respectively. There exists a bifurcation point between the values of 49 and 50, where the long-term behavior of the solution suddenly changes; a slight increase in the dose to $u_0 = 50$ leads to eradication of the biofilm. The same effect can also be achieved by slightly decreasing the frequency, but maintaining the dose $u_0 = 49$ (see Figure 2b)). Notice that when the frequency of dosing goes to zero or infinity the biofilm is eradicated, while in between the long-term limit is nonvanishing. Eradication in the case $\omega \to \infty$ directly follows from Theorem 2 (**how?**), but for the case $\omega \to 0+$ we only have numerical evidence but note that small ω means long intervals of nearly full dosing.

As we mentioned in the introduction, if both functions φ, ψ are chosen to be linear and we consider an on-off dosing $u^\mu(t) = u_0/\mu$ on $[0, \mu]$ and $u^\mu(t) = 0$ on $(\mu, 1]$ for a parameter $\mu \in (0, 1]$ then we obtain an unrealistic prediction for optimal dosing

strategy. As follows from Theorem 2, for large ω (i.e., small period P) the term $\mu\lambda$ in the equations (23) and (25) goes to zero as the parameter $\mu \to 0+$ with the consequences that the functionals $J(\mu)$ and $J(\mu_L)$ attain their minimum at $\mu = 0$. It follows that the optimal dosing strategy is a delta function (since $\lim_{\mu\to 0} u^\mu = u_0\delta$). One would instead expect saturation at a sufficiently high dosage.

This can be corrected by choosing the functions φ, ψ to be bounded, as in Figure 3b). In this case we can actually prove that the minimum is attained for a positive value of $\mu \leq 1$ (see Corollary 2 below). This indeed happens in Figure 3b) (where we use same parameters as in Figure 3a) but vary μ - the dosing ratio). Here the minimum of the functionals J, J_L is attained at all values $\mu \geq \mu_0 > 0$ for a threshold value $\mu_0 \approx 1/2$.

Corollary 2. *Let $u_0 > 0$. Assume that the functions φ and ψ are sublinear, i.e.,*

$$\lim_{x\to\infty} \frac{\varphi(x)}{x} = \lim_{x\to\infty} \frac{\psi(x)}{x} = 0.$$

Consider the functionals $J(\mu)$ and $J_L(\mu)$ for on-off dosing with the same average dose u_0 and for dosing time μ. Then the minimum of J and J_L is attained at some $\mu > 0$.

Proof. Let us analyze what happens in the equations (5)–(11) as $\mu \to 0+$. During the on time, $\varphi(B^\mu(t)) > 0$, $\psi(B^\mu(t)) > 0$, and during the off time, $\varphi(B^\mu(t)) = \psi(B^\mu(t)) = 0$. The assumption of sublinearity implies

$$\int_0^P \varphi(B^\mu)dt = \int_0^\mu \varphi\Big(\frac{u_0}{\mu}\frac{\cosh(\phi x)}{\cosh(\phi L^\mu(t))}\Big)dt \leq \mu\varphi\Big(\frac{u_0}{\mu}\Big),$$

so that $\lim_{\mu\to 0+} \varphi(B^\mu) = \lim_{\mu\to 0+} \psi(B^\mu) = 0$ in $L^1(0, P)$. Hence, the contributions of these two terms in equations (5)–(11) go to zero as $\mu \to 0+$. We can conclude that as $\mu \to 0+$, the functionals $J(\mu)$ and $J_L(\mu)$ converge to no-dosing value, i.e.,

$$\lim_{\mu\to 0} J(\mu) = \lim_{\mu\to 0} J_L(\mu) = \frac{\alpha}{\sigma}.$$

This means the minimum will never be attained at $\mu = 0$. □

Remark. For comparison, if for example φ is linear then $\varphi(B^\mu(t)) \to c\sum_{n\in\mathbb{Z}} \delta(nP)$, and hence the contribution of this term in the limit $\mu \to 0+$ cannot be ignored.

Figure 4a) plots the functionals J and J_L versus the frequency ω (on log scale) for on-off dosing. The two horizontal lines represents the limits $\omega \to 0+$ and $\omega \to \infty$ computed explicitly by invoking Theorems 2 and 3.

Unlike Figure 3b), where functionals J, J_L attain minimum at $\mu = 1$ (i.e. constant dosing), Figure 4b) shows a situation when on-off dosing is more advantageous

compared to constant dosing with an optimal value of μ strictly between 0 and 1. The gain of the functionals J, J_L over constant dosing is about 20% and 10%, respectively.

Figure 5 compares constant dosing to on-off dosing with the dosing ratio $\mu = 0.05$. The average dose u_0 is varied. Notice that for small dose constant dosing is always worse than on-off dosing. This is due to the fact that for small u_0 (and hence, small B) the term $\varphi(B)$ is almost linear and the effect of saturation of the bounded function φ is negligible (see Corollary 3). The situation changes if u_0 is large; for this set of parameters the best strategy is constant dosing. Indeed, recall that $\varphi(B) = \frac{M_\varphi u_0}{u_0+\mu k}$ for $B = \frac{u_0}{\mu}$ and $\mu \in (0, 1]$. Since $\mu k \approx 0$ and $M_\varphi \gg 1$, we obtain that $\varphi(B) \approx M_\varphi$ during the dosing time. The largest dosing time is when $\mu = 1$ (whole time), hence $\mu = 1$ is best – spiking dosage by setting $\mu < 1$ is of no advantage in the saturated case.

Corollary 3. *Let $\mu > 0$. Then for all $u_0 > 0$ sufficiently small, on-off dosing with average dose u_0 and dosing ratio μ is better than constant dosing with dose u_0.*

Proof. As stated above, if u_0 is small then $\varphi(B) \approx aB$ and $\psi(B) \approx a'B$ for some $a > 0$ and $a' > 0$. It follows that the functions Φ and Ψ appearing in the statement of Theorem 2 will be approximately equal to aB and $a'B$, respectively. Consider the linear case of the system (5)–(11), where the terms $\varphi(B), \psi(B)$ are replaced by aB and $a'B$. The first order expansion of the functional J_L about $u_0 = 0$ yields $J_L = L^{(0)} + L^{(1)}u_0 + O(u_0^2)$, where $L^{(0)} = \frac{\alpha}{\sigma}$ and

$$L^{(1)} = -\frac{a\gamma/(\lambda+\gamma) + a'\lambda/(\lambda+\gamma)}{\alpha\phi\cosh(\phi L^{(0)})} \int_0^{L^{(0)}} \frac{\sinh(\phi x)}{x} dx < 0.$$

(The analysis is similar for the other functional J). From this the claim follows. □

Note that "sufficiently small" dosage means that φ, ψ, are within their linear regimes.

4.3 A simple computational dosing experiment

As an example application, we consider the following question: given an adaptive infection, what is the preferable dosing strategy? That is, how should a daily dosage be divided into pills per day? From practical considerations, a patient might rather take one large pill than a number of smaller ones. However disinfection efficacy may or may not be well served by convenience although at least some evidence supports one per day dosing [32, 33, 35]. We won't present an in depth study of model predictions for this question here, but for example purposes we will discuss a comparison of a regime consisting of one full-dosed pill per day versus a regime of two half-dosed pills per day.

Figure 6 shows biofilm thickness L versus time for different values of the Thiele modulus ϕ (Thiele modulus larger than 1 indicates biofilm thickness large enough

to prevent full penetration; Thiele modulus less than 1 indicates full penetration is possible). We tested two scenarios - a concentrated dose at the beginning of the dosing period and two half-dosages given at the beginning and the in middle of the time period, both administered for the same length of dosing time as the concentrated dose. We observe that for thinner biofilms ($\phi = 0.8, \phi = 1$) a single concentrated dose is better than double dosing. Indeed, the functional J_L for the single dose corresponding to the ϕ's is about 28% and 23% smaller compared to the functional J_L for double dose. For thick biofilms ($\phi = 2$), however, the double dosing was slightly more advantageous compared to the single dose although differences were small and neither were very effective.

Figure 7 shows biofilm thickness L versus time for different values of the growth rate α. Recall that for no-dosing the steady-state is $L = \alpha/\sigma$. We conclude a similar phenomenon as before – for thinner biofilms ($\alpha = 0.5, \alpha = 1$) a single dose is better than double dosing with differences 12% and 33% corresponding to the α's. These results indicate that the success of dosing strategies is strongly correlated with the biofilm thickness and, under the assumptions made here, a small concentrated dosage is often more effective than multiple dosing. As a remark, the thin biofilm case (where a single concentrated pill is particularly effective) is rather similar to a planktonic infection in that "thin" means that biocide effectively penetrates, reaching all organisms. Thick biofilms, at least according to our model, are effectively defended against disinfection by adaptive response, pointing towards the importance of timeliness against bacterial infections. Indeed, mature biofilms are well known to be exhibit significant recalcitrance against antimicrobials.

5 Discussion

We have presented a mathematical model of bacterial adaptation, a resistance mechanism that has been observed in many experimental studies. The model is used to mathematically investigate different dosing protocols (constant, periodic and on and off) and to make predictions about their effectiveness. Therefore, we introduced two functionals J and J_L describing the average number of viable bacteria and average biofilm thickness and presented several optimization results.

The model predicts that for small doses, on-off dosing is more effective than constant dosing. Moreover, under certain assumptions, on-off dosing for a short period has a clear advantage over constant dosing regardless of the biocide dose. The optimal dosing ratio remains an open question; however, it would be possible to obtain an approximate numerical value by solving $\frac{dJ}{d\mu} = 0$ and taking higher order expansions of solutions with respect to μ.

While this model applies to bacterial biofilms, it serves as a framework for including planktonic systems in a time dependent biofilm model. This modification would require an additional equation for the substrate adjusted for a chemostat system and/or a batch culture. These questions will be investigated in future work.

Adaptive response has not been a subject of that much modeling to date, despite its potential importance in both the medical and industrial contexts. Part of the reason for this is the importance of the interconnection between adaptive response, a local biological phenomenon, and the spatial structure and dependence of biofilms, a coupling which introduces a number of mathematical complications. In this paper, we present several results aimed toward understanding and designing effective dosing protocols in the face of this microbial defense mechanism.

6 Acknowledgements

The authors would like to thank to Professor Phil S. Stewart for his valuable comments without which this manuscript could not have been written. Partial support was provided by NIH 5R01GM067245-02, EPSRC EP/F014589/1 and NSF upon agreement O112050.

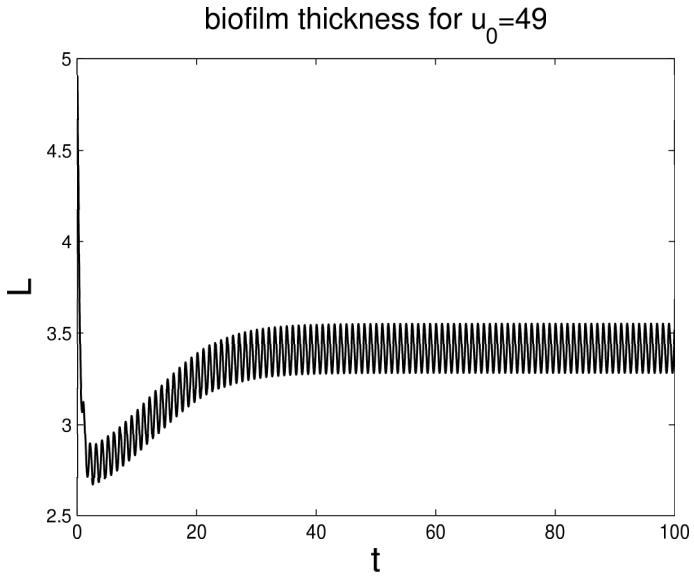

(a)

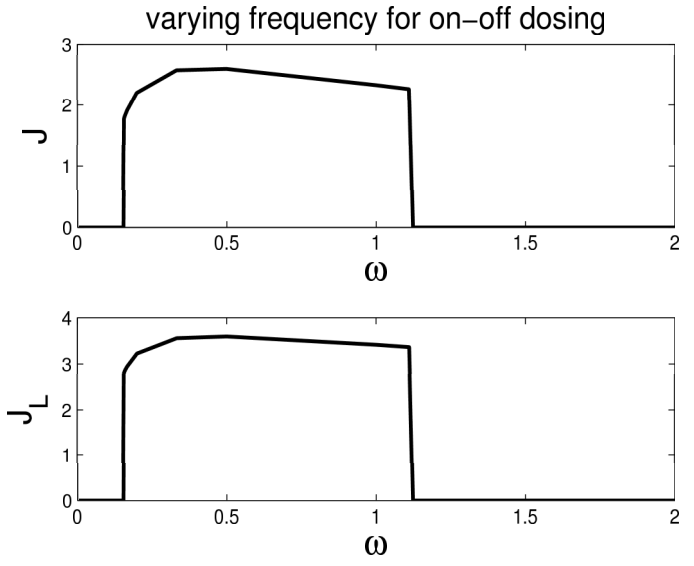

(b)

Figure 2: a) Biofilm thickness L with on-off dosing for values of the parameters $L(0) = 4.9, u_0 = 49, \phi = 1, \lambda = 2, \alpha = 2, \gamma = 0.2, \sigma = 0.4, M_\psi = 10, k = 100, M_\phi = 100, \mu = 0.5, P = 1$. b) Functionals J and J_L for different values of the frequency ω. The values of the other parameters are the same as in Figure 2 a).

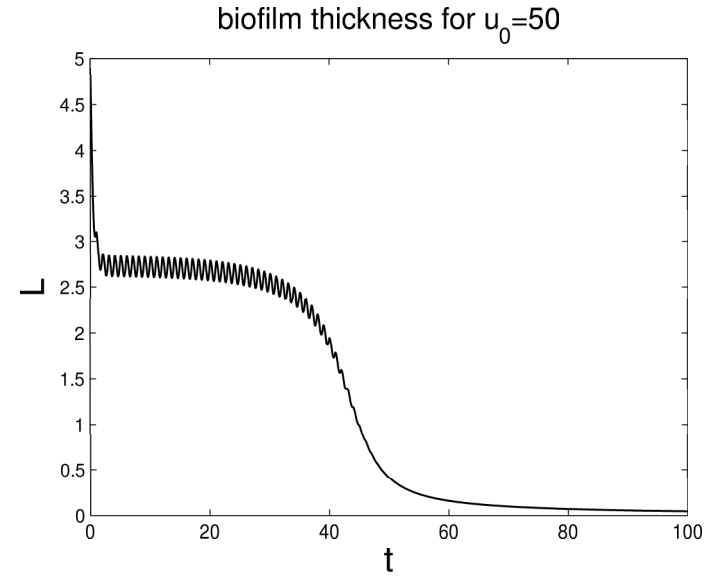

(a)

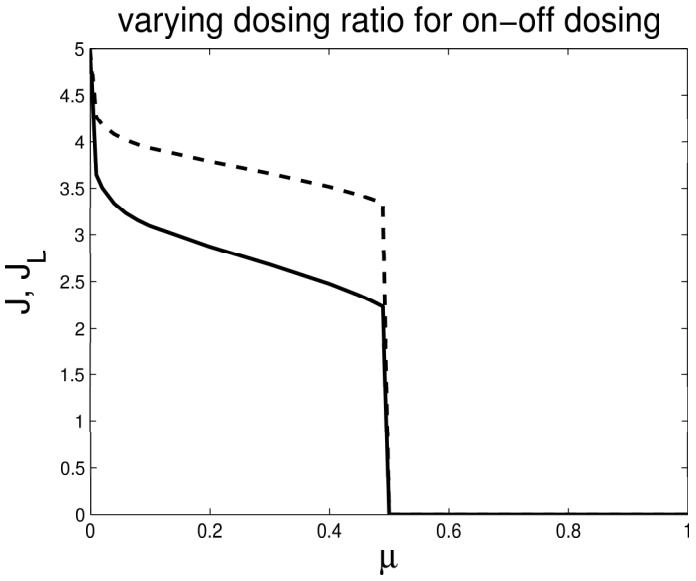

(b)

Figure 3: a) Biofilm thickness L with on-off dosing for values of the parameters $L(0) = 4.9, u_0 = 50, \phi = 1, \lambda = 2, \alpha = 2, \gamma = 0.2, \sigma = 0.4, M_\psi = 10, k = 100, M_\phi = 100, \mu = 0.5, P = 1$. b) Functionals J and J_L for different dosing time/period μ. The values of the other parameters are the same as in Figure 3 a).

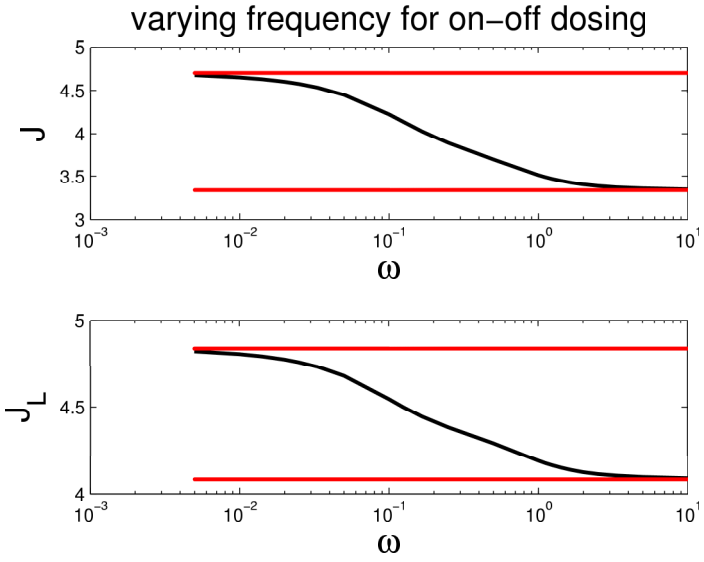

(a)

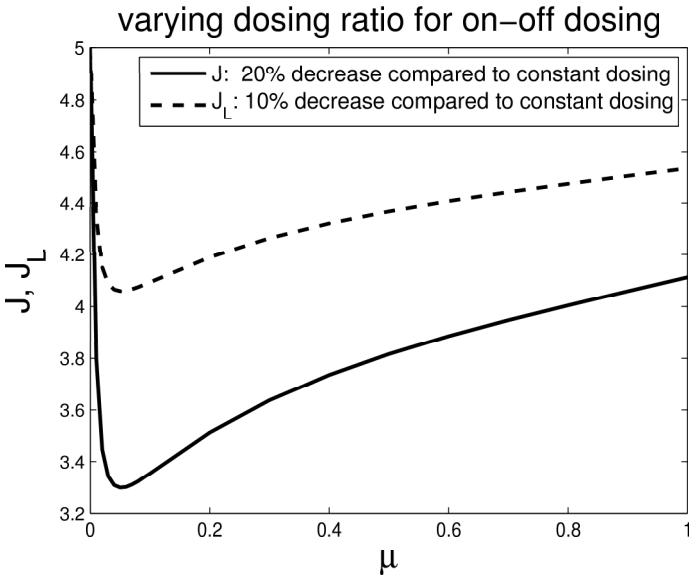

(b)

Figure 4: a) Functionals J and J_L for different values of the frequency ω. The values of the parameters are $L(0) = 1, u_0 = 1, \phi = 1, \lambda = 2, \alpha = 2, \gamma = 0.4, \sigma = 0.4, M_\psi = 0, k = 1, M_\phi = 35, \mu = 0.2$. The red horizontal lines, demarcating $\omega \to 0$ and $\omega \to \infty$, were computed explicitly based on Theorems 2 and 3. b) Functionals J and J_L for different ratios of the dosing time/period. The values of the parameters are $L(0) = 1, u_0 = 1, \phi = 1, \lambda = 2, \alpha = 2, \gamma = 0.4, \sigma = 0.4, M_\psi = 0, k = 1, M_\phi = 35, P = 1$.

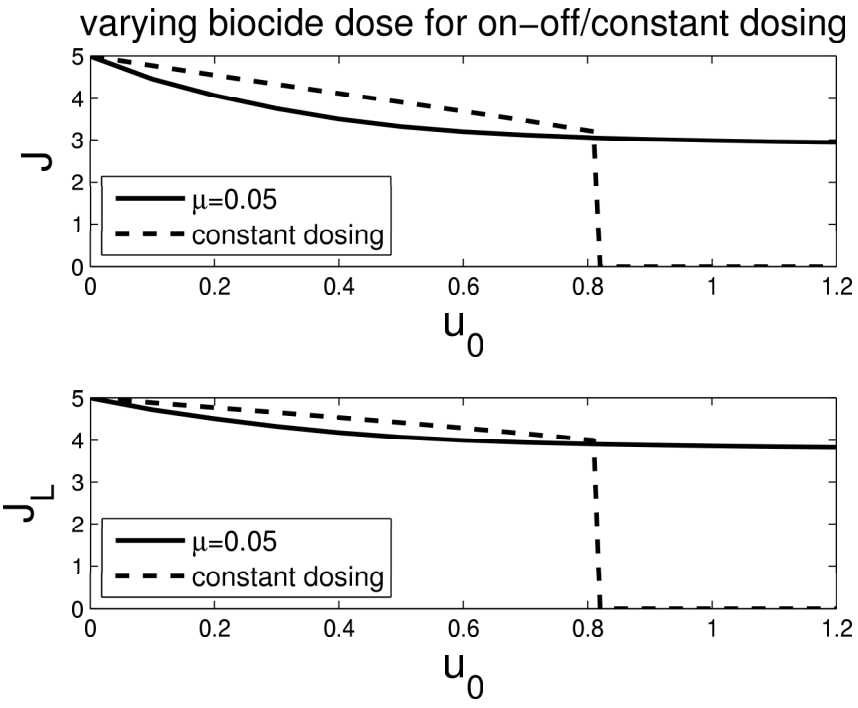

Figure 5: Functionals J and J_L for different values of the biocide dose u_0. The values of the parameters are $L(0) = 1, \phi = 1, \lambda = 2, \alpha = 2, \gamma = 0.4, \sigma = 0.4, M_\psi = 3.5, k = 1, M_\phi = 35$. The full curve corresponds to constant dosing with the same parameters. The dashed curve corresponds to on-off dosing with $\mu = 0.05, P = 1$.

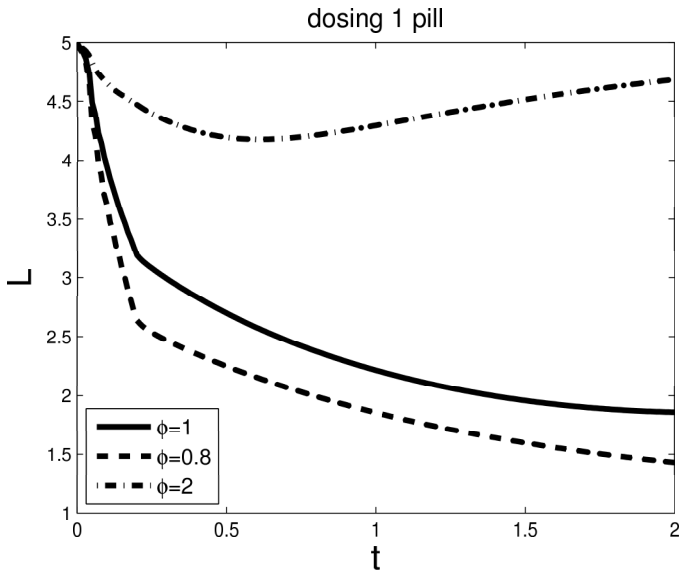

(a)

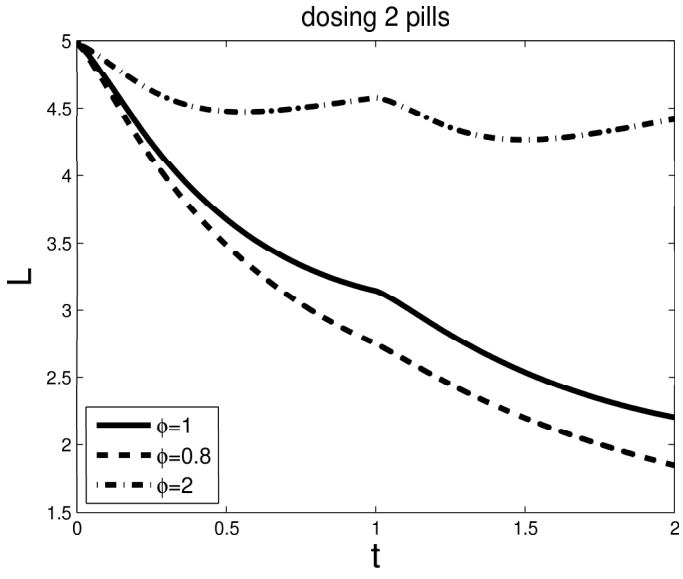

(b)

Figure 6: a) Biofilm thickness L when one pill is given at different values of the Thiele modulus ϕ. The values of the parameters are $L(0) = 5, u_0 = 12, \lambda = 2, \alpha = 1, \gamma = 0.2, \sigma = 0.2, M_\psi = 100, k = 100, M_\phi = 1000$. The time length is $T = 2$ and the dosing ratio is $\mu = 0.1$. b) Biofilm thickness L when 2 pills are given for different values of the Thiele modulus ϕ.

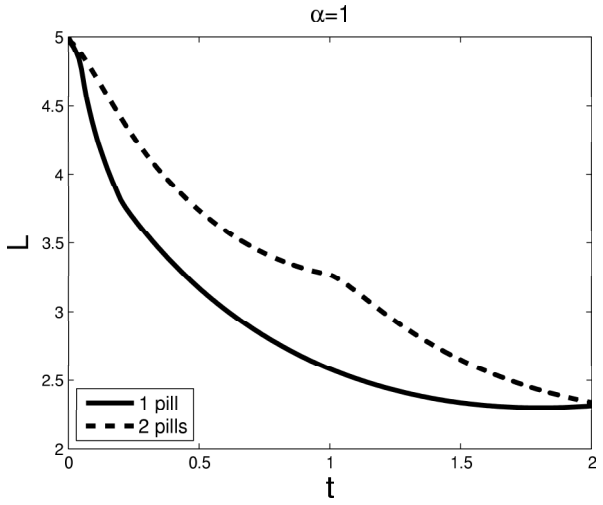

(a)

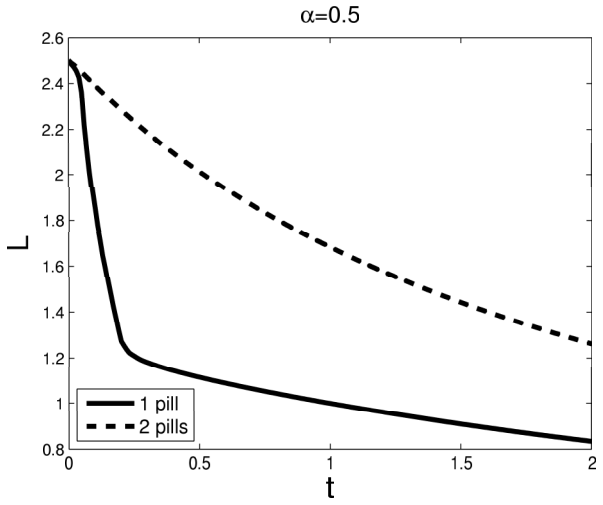

(b)

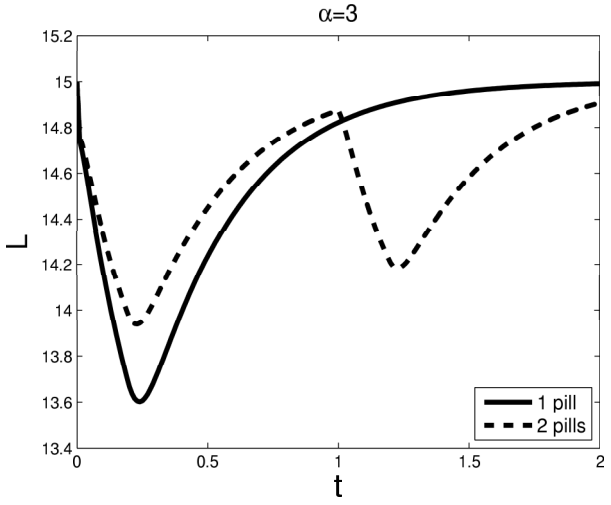

(c)

Figure 7: Biofilm thickness L when one and two pills are given for different values of the the growth rate α. The values of the parameters are $L(0) = \alpha/\sigma, u_0 = 10, \lambda = 2, \gamma = 0.2, \sigma = 0.2, M_\psi = 100, k = 100, M_\phi = 1000$. The time length is $T = 2$ and the dosing

References

[1] N. G. Cogan, R. Cortez & L. Fauci, Modeling physiological resistance in bacterial biofilms, Bull. of Math. Biol. **67**, 831-853, 2005.

[2] N. G. Cogan, Incorporating toxin hypothesis into a mathematical model of persister formation and dynamics, J. of. Theor. Biol. **248**, 340–349, 2007.

[3] N. G. Cogan, Effects of persister formation on bacterial response to dosing, J. Theor. Biol. **238**, 694–703, 2006.

[4] S. S. Sanderson & P.S. Stewart, Evidence of bacterial adaptation to monochloramine in *Pseudomonas aeruginosa* biofilms and evaluation of biocide action model, Biotechnology and Bioengineering **56**(2), 201–209, 1997.

[5] D.M. Grant & T.R. Brott, Biofilm dosing strategies for Biofilm Control in "Heat Exchanger Fouling and Cleaning: Fundamentals and Applications", P. Watkinson, H. Müller-Steinhagen & M. R. Malayeri Eds., ECI Symposium Series **RP1**, 2003.

[6] K.J. Grobe, J. Zahller & P.S. Stewart, Role of dose concentration in biocide efficacy against *Pseudomonas aeruginosa* biofilms, J. of Ind. Microbiol. and Biotechnol. **29**(1), 10–15, 2002.

[7] O. Steuernagel & D. Polani, 'Optimal strategies for fighting persister bugs', http://arxiv.org/PS_cache/q-bio/pdf/0512/0512003v1.pdf

[8] J. Pratten, A. W. Smith & M. Wilson, Response of single species biofilms and microcosm dental plaques to pulsing with chlorhexidine, J. of Antim. Chem. **42**, 453–459, 1998.

[9] B. Szomolay, Analysis of a moving boundary value problem arising in biofilm modelling, Math. Meth. Appl. Sci., DOI: 10.1002/mma.1000, 2008.

[10] B. Prakash, B. M. Veeregowda & G. Krishnappa, Biofilms: A survival strategy of bacteria, Current Science **85**(9), 2003.

[11] Research on microbial biofilms (PA-03-047), NIH, National Heart, Lung, and Blood Institute, 2002.

[12] W.G. Characklis, Microbial fouling, *Biofilms*, W.G. Characklis, K.C Marshall, eds. Wiley, New York, 523-584 (1990).

[13] G. Tchobanoglous, F.L. Burton, H.D Stensel, *Wastewater Engineering: Treatment and Reuse*, McGraw Hill, (2002).

[14] T.-F. C. Mah, B. Pitts, B. Pellock, G. C. Walker *et al.*, A genetic basis for Pseudomonas aeruginosa biofilm antibiotic resistance, Nature **426(**6964), 306–310, 2003.

[15] B.D. Hoyle, W.J. Costerton, Bacterial resistance to antibiotics: the role of biofilms, Prog. Drug Res. **37**, 91-105, 1991.

[16] T.-F. C. Mah & G. A. O'Toole, Mechanisms of biofilm resistance to antimicrobial agents, Trends Microbiol. **9**(1), 34–39, 2001.

[17] P. S. Stewart, Mechanism of antibiotic resistance in bacterial biofilms, Int. J. Med. Microbiol. **292**, 107–113, 2002.

[18] P. S. Stewart, M.A. Hamilton, B.R. Goldstein, B.T. Schneider, Modeling biocide action against biofilms, Biotech. Bioeng., **49**, 445-455, (1996).

[19] N. Bagge, M. Schuster, M. Hentzer, O. Ciofu *et al.*, *Pseudomonas aeruginosa* biofilms exposed to imipenem exhibit changes in global gene expression and beta-lactamase and alginate production, Antimicrob. Agents Chemother. **48**, 1175–1187, 2004.

[20] J. G. Elkins, D. J. Hassett, P. S. Stewart, H. P. Schweizer *et al.*, Protective role of catalase in *Pseudomonas aeruginosa* biofilm resistance to hydrogen peroxide, Appl. Environ. Microbiol. **65**, 4594-4600, 1999.

[21] B. Giwercman, E. T. H. Jensen, N. Høiby, A. Kharazmi *et al.*, Induction of β-lactamase production in *Pseudomonas aeruginosa* biofilm, Antimicrob. Agents Chemother. **35**, 1008–1010, 1991.

[22] B.Szomolay, I.Klapper, J.Dockery, P.S.Stewart, Adaptive responses to antimicrobial agents in biofilms, Environ. Microbiol. **7**, 1186-1191, 2005.

[23] L. R. Hoffman, D. A. D'Argenio, M. J. MacCross, Z. Zhang *et al.*, Aminoglycoside antibiotics induce bacterial biofilm formation, Nature **436**, 1171–1175, 2005.

[24] F. C. Sailer, B. M. Meberg & K. D. Young, β-lactam induction of colanic acid gene expression in *Escherichia coli*, FEMS Microbiol. Lett. **226**, 245–249, 2003.

[25] M. Whiteley, M. G. Bangera, R. E. Bumgarner *et al.*, Gene expression in *Pseudomonas aeruginosa* biofilms, Nature **413**, 860–864, 2001.

[26] K. Lewis, Riddle of biofilm resistance, Antimicrob Agents Chemo., **45**, 999-1007 (2001).

[27] I. Keren, N. Kaldalu, A. Spoering, Y. Wang, K. Lewis, Persister cells and tolerance to antimicrobials. FEMS Microbiol. Lett., **230**, 13-18 (2004).

[28] I. Klapper, P. Gilbert, B.P. Ayati, J. Dockery, P.S. Stewart, Senescence can explain microbial persistence. Microbiology, **153**, 3623-3630 (2007).

[29] B.P. Ayati, I. Klapper, A multiscale model of biofilm as a senescence-structured fluid. Multiscale Model. Sim., **6**, 347-365 (2007).

[30] Balaban, N.Q., Merrin, J., Chait, R., Kowalik, L., Leibler, S., Bacterial persistence as a phenotypic switch. *Science* **305**, 1622-1625 (2004).

[31] P.S. Stewart, A model of biofilm detachment. Biotech. Bioeng., **41**, 111-117 (1993).

[32] J. A. Karlowsky, S. A. Zelenitsky, G. G. Zhanel, Aminoglycoside adaptive resistance, Pharmacotheraphy **17**(3), 549–555 1997.

[33] M. L. Barclay, E. J. Begg, Aminoglycoside adaptive resistance: Importance for effective Dosage Regimens, Drugs **61**(6), 713–721, 2001.

[34] M. L. Barclay, E. J. Begg, S. T. Chambers, B. A. Peddie, The effect of aminoglycoside-induced adaptive resistance on the antibacterial activity of other antibiotics against *Pseudomonas aeruginosa in vitro*, J. Antim. Chem. **38**, 853–858, 1996.

[35] M. L. Barclay, E. J. Begg, S. T. Chambers, Adaptive resistance following single doses of gentamicin in a dynamic *in vitro* model, Antim. Agents and Chem. **36**(9), 1951–1957, 1992.

[36] W. M. Dunne, Effects of Subinhibitory Concentration of Vancomycin or Cefamandole on Biofilm Production by Coagulase-Negatice Staphylococci, Antim. Agents and Chem. **34**(3), 390–393, 1990.